

An Approach to Catalyst Design: Cyclopentadienyl-Titanium Phosphinimide Complexes in Ethylene Polymerization

Douglas W. Stephan,^{*,†} Jeffrey C. Stewart,[†] Frédéric Guérin,[†] Silke Courtenay,[†]
James Kickham,[†] Emily Hollink,[†] Chad Beddie,[†] Aaron Hoskin,[†] Todd Graham,[†]
Pingrong Wei,[†] Rupert E. v. H. Spence,[‡] Wei Xu,[‡] Linda Koch,[‡]
Xiaoliang Gao,[‡] and Daryll G. Harrison[‡]

*School of Physical Sciences, Chemistry and Biochemistry, University of Windsor,
Windsor, Ontario, Canada N9B 3P, and NOVA Chemicals Corporation, Research &
Technology Center, 2928 16 Street N.E., Calgary, Alberta, Canada T2E 7K7*

Received November 19, 2002

A strategy for polymerization catalyst design has been developed based on the steric and electronic analogy of bulky phosphinimides to cyclopentadienyl ligands. To this end, the family of complexes of the form (Cp[†])TiCl₂(NPR₃) has been prepared and characterized. Alkyl and aryl derivatives of these species have also been synthesized, and a number have been evaluated for use as catalyst precursors in olefin polymerization. The polymerization of ethylene has been examined employing several types of cocatalyst activators. Trends and patterns in the structure–activity relationship are discussed, and the implications for catalyst design are evaluated.

Introduction

Strategies for the development of new homogeneous olefin polymerization catalysts have resulted in the synthesis and exploration of a variety of new and interesting early transition metal complexes.^{1–3} For example, Ti and Zr complexes containing amido,^{4–6} diamido,^{7–12} amidinates,^{13–15} imidophosphonamides,¹⁶ pyridine-alkoxides,¹⁷ aryloxides,^{18–22} ketimides,^{23,24} borol-

lide,^{25,26} boratabenzene,^{27,28} pendant cyclopentadienyl borane ligands,²⁹ trimethylene,²⁸ cyclopentadienylborate,³⁰ diketimine,³¹ tropidinyl,³² tridentate,³³ and macrocyclic ligands³⁴ have been shown to exhibit appreciable catalytic activities. Nonetheless, perhaps the most commercially significant development since the advent of metallocene catalysts has been systems based on the so-called “constrained geometry catalyst” (CGC).^{35–43} This catalyst system evolved from a strategy of increas-

* Corresponding author. Fax: 519-973-7098. E-mail: stephan@uwindsor.ca.

[†] University of Windsor.

[‡] NOVA Chemicals Corporation.

(1) Britovsek, G. J. P.; Gibson, V. C.; Wass, D. F. *Angew. Chem.* **1999**, *38*, 428–447.

(2) Hlatky, G. G. *Coord. Chem. Rev.* **2000**, *199*, 235–329.

(3) Hlatky, G. G. *Chem. Rev.* **2000**, *100*, 1347–1376.

(4) Sinnema, P. J.; Okuda, J. *J. Organomet. Chem.* **2000**, *598*, 179–181.

(5) Shab, S. A. A.; Dorn, H.; Voigt, A.; Roesky, H. W.; Parisini, E.; Schmidt, H. G.; Noltemeyer, M. *Organometallics* **1996**, *15*, 3176.

(6) Nomura, K.; Fujii, K. *Organometallics* **2002**, *21*, 3042.

(7) Lorber, C.; Donnadieu, B.; Choukroun, R. *Organometallics* **2000**, *19*, 1963–1966.

(8) Scollard, J. D.; McConville, D. H. *J. Am. Chem. Soc.* **1996**, *118*, 10008–10009.

(9) Scollard, J. D.; McConville, D. H.; Vittal, J. J. *Organometallics* **1995**, *14*, 5478–5480.

(10) Warren, T. H.; Schrock, R. R.; Davis, W. M. *Organometallics* **1998**, *17*, 308–321.

(11) Cloke, F. G. N.; Geldach, T. J.; Hitchcock, P. B.; Love, J. B. *J. Organomet. Chem.* **1996**, *506*, 343–345.

(12) Bazan, G. C.; Cotter, W. D.; Komon, Z. J. A.; Lee, R. A.; Lachicotte, R. J. *J. Am. Chem. Soc.* **2000**, *122*, 1371–1380.

(13) Jayaratne, K. C.; Sita, L. R. *J. Am. Chem. Soc.* **2000**, *122*, 958–959.

(14) Jayaratne, K. C.; Koarron, R. J.; Hemmings, D. A.; Sita, L. R.; Babcock, R. *J. Am. Chem. Soc.* **2000**, *122*, 10490.

(15) Richter, J.; Edelmann, F. T.; Noltemeyer, M.; Schmidt, H.-G.; Shmulinson, M.; Eisen, M. S. *J. Mol. Catal. A: Chem.* **1998**, *130*, 149–162.

(16) Vollmerhaus, R.; Shao, P.; Taylor, N. J.; Collins, S. *Organometallics* **1999**, *18*, 2731–2733.

(17) Doherty, S.; Errington, R. J.; Jarvis, A. P.; Collins, S.; Clegg, W.; Elsegood, M. R. *J. Organometallics* **1998**, *17*, 3408.

(18) Nomura, K.; Naga, N.; Miki, M.; Yanagi, K.; Imai, A. *Organometallics* **1998**, *17*, 2152–2154.

(19) Tsukahara, T.; Swenson, D. C.; Jordan, R. F. *Organometallics* **1997**, *16*, 3303–3313.

(20) Van Der Linden, A.; Schaverien, C. J.; Meijboom, N.; Ganter, C.; Orpen, A. G. *J. Am. Chem. Soc.* **1995**, *117*, 3008–3021.

(21) Nomura, K.; Naga, N.; Miki, M.; Yanagi, K. *Macromolecules* **1998**, *31*, 7588.

(22) Antinolo, A.; Carrillo-Hermosilla, F.; Corrochano, A. E.; Fernandez-Baeza, J.; Lara-Sanchez, A.; Ribeiro, M. R.; Lanfranchi, M.; Otero, A.; Pellinghelli, M. A.; Portela, M. F.; Saritos, J. V. *Organometallics* **2000**, *19*, 2837.

(23) McMeeking, J.; Gao, X.; Spence, R. E. v. H.; Brown, S. J.; Jeremic, D. NOVA Chemicals: USA 6114481, 2000.

(24) Kretschmer, W. P.; Dijkhnis, C.; Meetsma, A.; Hessen, B. T.; Teuben, J. H. *Chem. Commun.* **2002**, 608.

(25) Bazan, G. C.; Schaefer, W. P.; Bercaw, J. E. *Organometallics* **1993**, *12*, 2126.

(26) Bazan, G. C.; Donnelly, S. J.; Ridriguez, G. *J. Am. Chem. Soc.* **1995**, *117*, 2671–2672.

(27) Bazan, G. C.; Rodriguez, G.; Ashe, A. J., III; Al-Ahmad, S.; Muller, C. *J. Am. Chem. Soc.* **1996**, *118*, 2291–2292.

(28) Bazan, G. C.; Rodriguez, G. *Organometallics* **1997**, *16*, 2492–2494.

(29) Spence, R. E. v. H.; Piers, W. E. *Organometallics* **1995**, *14*, 4617–4624.

(30) Sun, Y.; Spence, R. E. v. H.; Piers, W. E.; Parvez, M.; Yap, G. P. A. *J. Am. Chem. Soc.* **1997**, *119*, 5132–5143.

(31) Vollmerhaus, R.; Rahim, M.; Tomaszewski, R.; Xin, S.; Taylor, N. J.; Collins, S. *Organometallics* **2000**, *19*, 2161–2169.

(32) Skoog, S. J.; Mateo, C.; Lavoie, G. G.; Hollander, F. J.; Bergman, R. G. *Organometallics* **2000**, *19*, 1406–1421.

(33) Okuda, J.; Eberle, T.; Spaniol, T. P.; Piquet-Faure, V. *J. Organomet. Chem.* **2000**, *591*, 127–137.

(34) Fokken, S.; Spaniol, T. P.; Kang, H.-C.; Massa, W.; Okuda, J. *Organometallics* **1996**, *15*, 5069–5072.

ing the exposure of the metal center by the incorporation of a constrained chelating cyclopentadienyl-amide ligand.

In developing our own approach to catalyst design, we noted the work of Wolczanski et al.,⁴⁴ who described the steric analogy between the tri-*tert*-butylmethoxide (tritox) and cyclopentadienyl ligands. In addition, we took notice of the electronic analogy between phosphinimide and cyclopentadienyl ligands described by Dehnicke et al.^{45–48} As phosphinimide ligands are structurally related to Wolczanski's "tritox", we recognized that bulky phosphinimides offer both steric and electronic analogies to the cyclopentadienyl ligand. Moreover, these ligands are easily modified, providing the opportunity for systematic studies of structure–activity relationships and they provide the powerful probe associated with ³¹P NMR spectroscopy.⁴⁹ In this article, we detail the synthesis and characterization of a family of complexes of the form Cp[†]TiCl₂(NPR₃) that include such phosphinimide ligands. In addition, a number of alkyl and aryl derivatives are described. These species are shown to act as precursors to effective ethylene polymerization catalysts. This family of compounds yields active catalysts, although the levels of activity depend both on the precise details of the ligands and on the mode of activation. Trends in the structure–property–activity relationships are evaluated and discussed. A preliminary account of some of the results presented herein has previously been published.⁵⁰

Experimental Section

General Data. All preparations were done under an atmosphere of dry, O₂-free N₂ employing both Schlenk line techniques and Innovative Technologies, Braun, or Vacuum Atmospheres inert atmosphere gloveboxes. Solvents were purified employing Grubbs' type column systems manufactured by Innovative Technology. ¹H and ¹³C{¹H} NMR spectra were recorded on Bruker Avance-300 and -500 spectrometers operating at 300 and 500 MHz, respectively. Trace amounts of protonated solvents were used as references, and chemical shifts in ppm are reported relative to SiMe₄. ³¹P{¹H} NMR, ¹¹B{¹H} NMR, and ¹⁹F NMR spectra were recorded on a Bruker

Avance-300 and are referenced to 85% H₃PO₄, saturated NaBH₄/H₂O, and 80% CFCl₃ in CDCl₃, respectively. Unless otherwise stated, all spectra were recorded at 25 °C in *d*₆-benzene. Guelph Chemical Laboratories performed combustion analyses. In a very few cases, despite repeated analyses and the use of added oxidant, C analyses yielded deviations from calculated values. We attribute this to partial formation of TiC during combustion of the Ti-organometallic derivatives. The compounds R₃PNSiMe₃, CpTiCl₃, Cp*TiCl₃, (indenyl)TiCl₃, (*t*-BuC₅H₄)TiCl₃, (*n*-BuC₅H₄)TiCl₃, (indenyl)Ti(NP*t*-Bu₃)Cl₂ (**24**), and (Indenyl)Ti(NP*t*-Bu₃)Me₂ (**41**) were prepared via published methods.^{46,51,52} The precursor phosphines and N₃SiMe₃ were purchased from either the Strem Chemical or Aldrich Chemical Companies.

Synthesis of R₃PNSiMe₃ (R = Et **1, Cy **2**, *i*-Pr **3**, *t*-Bu **4**, Ph **5**, *p*-MeC₆H₄ **6**, *p*-CF₃C₆H₄ **7**, *p*-FC₆H₄ **8**, *p*-MeOC₆H₄ **9**).** These compounds were prepared in a fashion similar to that described in the literature for **5** with only minor modifications to the published procedure, other than substitution of the appropriate phosphine precursor. Thus, a single preparation is detailed. Me₃SiN₃ (2.95 g, 10.7 mmol) was added to 3.00 g (10.7 mmol) of Et₃P to give an off-white slush. Heating with stirring for 5 h at 80 °C initially produced a bubbling, light yellow liquid, which became a darker yellow, clear liquid after 20 min. Cooling yielded a light brown, waxy solid, which was recrystallized at –35 °C from MeCN (50 mL) to give 1.75 g (80%) of the cream-colored solid product **1**. ³¹P{¹H} NMR: 15.0. ¹H NMR: 1.12 (m, 6H, CH₂); 0.84 (m, 9H, Me); 0.34 (s, 9H, SiMe₃). ¹³C{¹H} NMR: 21.9 (d, ¹J_{PC} = 67 Hz, PCH₂); 6.4 (CH₂Me), 5.0 (SiMe₃). **2** (93%): ³¹P{¹H} NMR: 17.0. ¹H NMR: 1.88–1.09 (m, 33H, Cy); 0.43 (s, 9H, SiMe₃). ¹³C{¹H}: 37.1 (d, ¹J_{PC} = 48 Hz, PCH); 27.4 (d, ²J_{PC} = 12 Hz, CH₂), 27.3, 26.9 (CH₂); 5.3 (SiMe₃). **3** (87%): ³¹P{¹H} NMR: 24.6. ¹H NMR: 1.62 (m, 3H, CHMe₂); 0.93 (m, 18H, CHMe₂); 0.34 (s, 9H, SiMe₃). ¹³C{¹H} NMR: 26.1 (d, ¹J_{PC} = 63 Hz, PCHMe₂); 17.2 (PCHMe₂); 5.0 (SiMe₃). **4** (86%): ³¹P{¹H} NMR: 32.4. ¹H NMR: 1.17 (d, ³J_{PH} = 13 Hz, 27H, PCMe₃); 0.4 (s, 9H, SiMe₃). ¹³C{¹H} NMR: 39.9 (d, ¹J_{PC} = 55 Hz, PCMe₃); 29.6 (PCMe₃); 4.8 (SiMe₃). Anal. Calcd for C₁₅H₃₆NPSi: C, 62.21; H, 12.56; N, 4.84. Found: C, 62.12; H, 12.40; N, 4.85. **5**: ³¹P{¹H} NMR: –0.5. ¹H NMR: 7.72 (m, 6H, Ph); 7.03 (m, 9H, Ph); 0.36 (s, 9H, SiMe₃). ¹³C{¹H} NMR: 136.7, 135.4, 132.3 (d, ²J_{PC} = 9 Hz, Ph); 128.8 (d, ³J_{PC} = 6 Hz, Ph); 4.43 (SiMe₃). **6** (93%): ³¹P{¹H} NMR: 0.04. ¹H NMR: 7.75 (dd, ³J_{HH} = 8 Hz, ³J_{PH} = 12 Hz, 6H, C₆H₄Me); 6.92 (d, ³J_{HH} = 8 Hz, 6H, C₆H₄Me); 1.99 (s, 9H, C₆H₄Me); 0.42 (s, 9H, SiMe₃). ¹³C{¹H} NMR: 140.9, 134.2 (C₆H₄Me); 132.4 (d, ³J_{PC} = 11 Hz, C₆H₄Me); 129.1 (d, ²J_{PC} = 13 Hz, C₆H₄Me); 21.2 (C₆H₄Me); 4.5 (SiMe₃). Anal. Calcd for C₂₄H₃₀NPSi: C, 73.62; H, 7.72; N, 3.58. Found: C, 72.90; H, 7.93; N, 3.88. **7** (92%): ³¹P{¹H} NMR: –5.5. ¹H NMR: 7.38 (dd, ³J_{HH} = 8 Hz, ³J_{PH} = 12 Hz, 6H, C₆H₄CF₃); 7.25 (d, ³J_{HH} = 8 Hz, 6H, C₆H₄CF₃); 0.27 (s, 9H, SiMe₃). ¹³C{¹H} NMR: 139.3 (C₆H₄CF₃), 137.9, 132.5 (C₆H₄CF₃); 133.3 (d, ²J_{PC} = 35 Hz, *p*-C₆H₄CF₃); 125.5 (d, ³J_{FC} = 13 Hz, *m*-C₆H₄CF₃); 4.0 (SiMe₃). ¹⁹F NMR: 14.8. Anal. Calcd for C₂₄H₂₁F₉NPSi: C, 65.59; H, 4.81; N, 3.19. Found: C, 65.23; H, 4.55; N, 3.07. **8** (93%): ³¹P{¹H} NMR: –3.8. ¹H NMR: 7.41 (m, 6H, C₆H₄F); 6.69 (dd, ³J_{HH} = 8 Hz, ³J_{PH} = 2 Hz, 6H, C₆H₄F); 0.29 (9H, SiMe₃). ¹³C{¹H} NMR: 164.8 (d, ¹J_{FC} = 253 Hz, C₆H₄–F); 134.4 (dd, ²J_{PC} = 12 Hz, ³J_{FC} = 8 Hz, *o*-C₆H₄); 131.5 (dd, ⁴J_{FC} = 4 Hz, ¹J_{PC} = 106 Hz, *ipso*-C₆H₄F); 115.7 (dd, ³J_{PC} = 13 Hz, ²J_{FC} = 21 Hz, *m*-C₆H₄F); 4.2 (d, ³J_{PC} = 4 Hz, SiMe₃). ¹⁹F NMR: –30.6. Anal. Calcd for C₂₁H₂₁F₃NPSi: C, 62.51; H, 5.26; N, 3.47. Found: C, 62.55; H, 5.32; N, 3.20. **9** (89%): ³¹P{¹H} NMR: –0.7. ¹H NMR: 7.75 (dd, ³J_{HH} = 8 Hz, ³J_{PH} = 12 Hz, 6H, C₆H₄); 6.71 (dd, ³J_{HH} = 8 Hz, ⁴J_{PH} = 2 Hz, 6H, C₆H₄); 3.21 (s, 9H, MeO); 0.45 (s, 9H, SiMe₃). ¹³C{¹H} NMR: 162.0 (d, ⁴J_{PC} = 4 Hz, *p*-C₆H₄); 134.1 (d, ³J_{PC} = 12 Hz, *m*-C₆H₄); 128.9, 113.9 (d, ²J_{PC} = 13 Hz); 54.7 (OMe); 4.64 (SiMe₃).

(51) Samuel, E.; Rausch, M. D. *J. Am. Chem. Soc.* **1973**, *95*, 6263.

(52) Guerin, F.; Beddie, C. L.; Stephan, D. W.; Spence, R. E. v. H.; Wurz, R. *Organometallics* **2001**, *20*, 3466–3471.

(35) Shapiro, P. J.; Bunel, E.; Schaefer, W. P.; Bercaw, J. E. *Organometallics* **1990**, *9*, 867–869.

(36) Chen, Y.-X.; Marks, T. J. *Organometallics* **1997**, *16*, 3649–3657.

(37) Tian, S.; Arredondo, V. M.; Stern, C. L.; Marks, T. J. *Organometallics* **1999**, *18*, 2568–2570.

(38) Deck, P. A.; Beswick, C. L.; Marks, T. J. *J. Am. Chem. Soc.* **1998**, *120*, 1772–1784.

(39) Woo, T. K.; Margl, P. M.; Lohrenz, J. C. W.; Blochl, P. E.; Ziegler, T. *J. Am. Chem. Soc.* **1996**, *118*, 13021–13030.

(40) Shapiro, P. J.; Cotter, W. D.; Schaefer, W. P.; Labinger, J. A.; Bercaw, J. E. *J. Am. Chem. Soc.* **1994**, *116*, 4623–4640.

(41) Devore, D. D.; Timmers, F. J.; Hasha, D. L.; Rosen, R. K.; Marks, T. J.; Deck, P. A.; Stern, C. L. *Organometallics* **1995**, *14*, 3132–3134.

(42) Lindsay, K. F. *Mod. Plast.* **1993**, 82.

(43) Stevens, J. C. In *Catalyst Design for Taylor-made Polyolefins, Studies in Surface Science and Catalysis*, Soga, K., Terano, M., Eds.; Elsevier: Amsterdam, 1994; Vol. 89, pp 277–284.

(44) Lubben, T. V.; Wolczanski, P. T.; Van Duyne, G. D. *Organometallics* **1984**, *3*, 977–983.

(45) Anfang, S.; Harms, K.; Weller, F.; Borgmeier, O.; Lueken, H.; Schilder, H.; Dehnicke, K. Z. *Anorg. Allg. Chem.* **1998**, *624*, 159–166.

(46) Dehnicke, K.; Weller, F. *Coord. Chem. Rev.* **1997**, *158*, 103–169.

(47) Dehnicke, K.; Krieger, M.; Massa, W. *Coord. Chem. Rev.* **1999**, *182*, 19–65.

(48) Dehnicke, K.; Straehle, J. *Polyhedron* **1989**, *8*, 707–726.

(49) Kickham, J. E.; Guerin, F.; Stephan, D. W. *J. Am. Chem. Soc.* **2002**, *124*, 11486–11494.

(50) Stephan, D. W.; Stewart, J. C.; Guerin, F.; Spence, R. E. v. H.; Xu, W.; Harrison, D. G. *Organometallics* **1999**, *18*, 1116–1118.

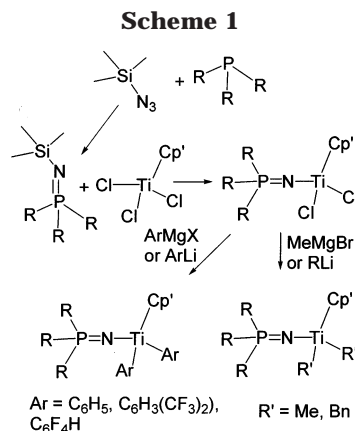
Table 1. Compound Numbering

compound type	Cp'	R
R ₃ PNSiMe ₃		Et 1 , Cy 2 , <i>i</i> -Pr 3 , <i>t</i> -Bu 4 , Ph 5 , <i>p</i> -MeC ₆ H ₄ 6 , <i>p</i> -CF ₃ C ₆ H ₄ 7 , <i>p</i> -FC ₆ H ₄ 8 , <i>p</i> -CH ₃ OC ₆ H ₄ 9
Cp'Ti(NPR ₃)Cl ₂	C ₅ H ₅	Et 10 , Cy 11 , <i>i</i> -Pr 12 , <i>t</i> -Bu 13 , Ph 14 , <i>p</i> -MeC ₆ H ₄ 15 , <i>p</i> -CF ₃ C ₆ H ₄ 16 , <i>p</i> -FC ₆ H ₄ 17 , <i>p</i> -CH ₃ OC ₆ H ₄ 18
	Me ₃ SiC ₅ H ₄	<i>i</i> -Pr 19 , <i>t</i> -Bu 20
	C ₅ Me ₅	<i>i</i> -Pr 21 , <i>t</i> -Bu 22
	Indenyl	<i>i</i> -Pr 23 , <i>t</i> -Bu 24
	<i>t</i> -BuC ₅ H ₄	Cy 25 , <i>i</i> -Pr 26 , <i>t</i> -Bu 27
	<i>n</i> -BuC ₅ H ₄	<i>t</i> -Bu 28
	Ph ₄ C ₅ H	<i>t</i> -Bu 29
Cp'Ti(NPR ₃)Me ₂	C ₅ H ₅	Cy 30 , <i>i</i> -Pr 31 , <i>t</i> -Bu 32 , Ph 33 , <i>p</i> -MeC ₆ H ₄ 34 , <i>p</i> -CF ₃ C ₆ H ₄ 35 , <i>p</i> -FC ₆ H ₄ 36 , <i>p</i> -CH ₃ OC ₆ H ₄ 37
	C ₅ Me ₅	<i>i</i> -Pr 38 , <i>t</i> -Bu 39
	Indenyl	<i>i</i> -Pr 40 , <i>t</i> -Bu 41
	<i>t</i> -BuC ₅ H ₄	Cy 42 , <i>i</i> -Pr 43 , <i>t</i> -Bu 44
	Ph ₄ C ₅ H	<i>t</i> -Bu 45
CpTi(NPR ₃)Bn ₂		Cy 46 , <i>i</i> -Pr 47 , <i>t</i> -Bu 48 , Ph 49 , <i>p</i> -MeC ₆ H ₄ 50 , <i>p</i> -CF ₃ C ₆ H ₄ 51 , <i>p</i> -FC ₆ H ₄ 52 , <i>p</i> -CH ₃ OC ₆ H ₄ 53
CpTi(NPR ₃)Ph ₂		Cy 54 , <i>i</i> -Pr 55 , <i>t</i> -Bu 56 , Ph 57
CpTi(NPR ₃)(C ₆ H ₃ -3,5-(CF ₃) ₂) ₂		Cy 58 , Ph 59
CpTi(NPR ₃)(C ₆ H-2,3,4,5-F ₄) ₂		Ph 60
CpTi(NPR ₃)(CH ₂ Si(CH ₃) ₃) ₂		<i>t</i> -Bu 61 Ph 62
CpTi(NPR ₃)Cl(O-2,6- <i>i</i> -Pr ₂ C ₆ H ₃)		<i>t</i> -Bu 63

subsequently washed with MeOH and dried at 100 °C for at least 24 h prior to weighing.

X-ray Data Collection and Reduction. X-ray quality crystals were obtained directly from the preparations as described above. The crystals were manipulated and mounted in capillaries in a glovebox, thus maintaining a dry, O₂-free environment for each crystal. Diffraction experiments were performed on a Siemens SMART System CCD diffractometer. The data were collected for a hemisphere of data in 1329 frames with 10 s exposure times. Crystal data are summarized in Table 2. The observed extinctions were consistent with the space groups in each case. A measure of decay was obtained by re-collecting the first 50 frames of each data set. The intensities of reflections within these frames showed no statistically significant change over the duration of the data collections. An empirical absorption correction based on redundant data was applied to each data set. Subsequent solution and refinement was performed using the SHELXTL solution package.

Structure Solution and Refinement. Non-hydrogen atomic scattering factors were taken from the literature tabulations.⁵³ The heavy atom positions were determined using direct methods. The remaining non-hydrogen atoms were located from successive difference Fourier map calculations. The refinements were carried out by using full-matrix least-squares techniques on F_o , minimizing the function $w(F_o - F_c)^2$ where the weight w is defined as $4F_o^2/2\sigma(F_o^2)$ and F_o and F_c are the observed and calculated structure factor amplitudes. For non-centrosymmetric space groups, the correct enantiomorph was confirmed by data inversion and refinement. In the final cycles of each refinement, all non-hydrogen atoms were assigned anisotropic temperature factors. Carbon-bound hydrogen atom positions were calculated and allowed to ride on the carbon to which they are bonded assuming a C–H bond length of 0.95 Å. Hydrogen atom temperature factors were fixed at 1.10 times the isotropic temperature factor of the carbon atom to which they are bonded. The hydrogen atom contributions were calculated, but not refined. The final values of refinement parameters are given in Table 2. Positional parameters, hydrogen atom parameters, thermal parameters, and bond distances and angles have been deposited as Supporting Information.



Results and Discussion

Synthesis and Characterization. Numerous phosphines can be oxidized to the corresponding phosphinimine derivative by reaction with Me₃SiN₃.⁴⁶ In this manner, the series of compounds R₃PNSiMe₃ (Table 1) have been prepared. Several of these phosphinimines have been previously prepared,⁴⁶ although the present report provides full NMR spectroscopic data for these ligand precursors. Subsequent reaction with Cp'TiCl₃ provides facile access to the corresponding series of complexes of the form Cp'Ti(NPR₃)Cl₂ (Table 1). Employing the appropriate precursors, this family of compounds can be readily extended to include substitution on the cyclopentadienyl ligand or Cp alternatives. In this fashion the species (Cp')Ti(NPR₃)Cl₂ (Table 1) were also readily prepared. The synthetic routes are generalized in Scheme 1. All of these species are obtained in high yield and are readily purified by recrystallization.

Compounds **11–13**, **21–23**, **27**, and **28** have been characterized crystallographically. Representative structures of the dichloride derivatives are presented in Figures 1–5. In all cases the Ti adopts a pseudo-tetrahedral geometry with the cyclopentadienyl ligand or its analogue, the two chlorides and the phosphinimide nitrogen completing the coordination sphere. It is noteworthy that the indenyl group in **23** and the

(53) Cromer, D. T.; Mann, J. B. *Acta Crystallogr. A* **1968**, *A24*, 321–324.

Table 2. Crystallographic Parameters^a

	11	12	13	21
formula	C ₂₃ H ₃₈ Cl ₂ NPTi	C ₁₄ H ₂₆ Cl ₂ NPTi	C _{20.5} H _{35.5} Cl ₂ NPTi	C ₁₉ H ₃₆ Cl ₂ NPTi
fw	478.31	358.13	445.77	428.26
<i>a</i> (Å)	8.8309(6)	14.4159(8)	33.537(10)	13.064(3)
<i>b</i> (Å)	18.8687(12)	16.1783(9)	8.532(3)	12.971(3)
<i>c</i> (Å)	14.8404(10)	15.8076(9)	17.963(5)	13.928(3)
β (deg)	90.7500(10)	91.4547(11)	110.349(7)	102.29(2)
cryst syst	monoclinic	monoclinic	monoclinic	monoclinic
space group	<i>P2</i> (1)/ <i>c</i>	<i>P2</i> (1)/ <i>c</i>	<i>C2</i> / <i>c</i>	<i>P2</i> (1)/ <i>n</i>
vol (Å ³)	2472.6(3)	3685.5(4)	4819(2)	2306.1(9)
<i>D</i> _{calcd} (g cm ⁻³)	1.285	1.291	1.229	1.234
<i>Z</i>	4	8	8	4
abs coeff, μ , mm ⁻¹	0.636	0.830	0.648	0.674
no. of data collected	9328	14139	1695	1862
no. of data $F_o^2 > 3\sigma(F_o^2)$	3524	6258	1634	1262
no. of variables	253	343	215	217
<i>R</i> (%)	0.0462	0.0472	0.1239	0.0363
<i>R</i> _w (%)	0.1110	0.0902	0.2727	0.0938
goodness of fit	1.036	0.832	1.341	0.757

	22	23	27
formula	C ₂₂ H ₄₂ Cl ₂ NPTi	C ₁₈ H ₂₈ Cl ₂ NPTi	C ₂₁ H ₄₀ Cl ₂ NPTi
fw	470.34	408.18	456.31
<i>a</i> (Å)	11.6734(6)	17.160(2)	8.4136(2)
<i>b</i> (Å)	16.6150(9)	13.119(2)	15.8989(2)
<i>c</i> (Å)	13.614(7)	18.646(4)	19.3131(4)
β (deg)	98.2953(11)		96.8610(10)
cryst syst	monoclinic	orthorhombic	monoclinic
space group	<i>P2</i> (1)/ <i>n</i>	<i>Pca</i> 2(1)	<i>P2</i> (1)/ <i>c</i>
vol (Å ³)	2612.9(14)	4197.5(12)	2564.95(9)
<i>D</i> _{calcd} (g cm ⁻³)	1.196	1.292	1.182
<i>Z</i>	4	8	4
abs coeff, μ , mm ⁻¹	0.601	0.738	0.610
no. of data collected	12 914	20 359	12 749
data $F_o^2 > 3\sigma(F_o^2)$	4553	7302	4447
no. of variables	244	415	235
<i>R</i> (%)	0.0598	0.0394	0.0530
<i>R</i> _w (%)	0.1604	0.0620	0.1531
goodness of fit	1.061	0.764	1.030

	28	56	62	63
formula	C ₂₁ H ₄₀ Cl ₂ NPTi	C ₂₉ H ₄₂ NPTi	C ₃₁ H ₄₂ NPSi ₂ Ti	C ₂₉ H ₄₀ ClNOPTi
fw	456.31	483.51	563.71	542.01
<i>a</i> (Å)	15.472(4)	18.54800	11.069(5)	17.777(6)
<i>b</i> (Å)	8.5317(13)	15.0094	12.798(6)	10.7647(15)
<i>c</i> (Å)	18.928(4)	19.65940(10)	12.887(6)	32.068(7)
α (deg)			100.195(9)	
β (deg)	100.973(12)		100.894(9)	
γ (deg)			105.726(9)	
cryst syst	monoclinic	orthorhombic	triclinic	orthorhombic
space group	<i>P2</i> (1)/ <i>n</i>	<i>Pbca</i>	<i>P1</i>	<i>Pca</i> 2(1)
vol (Å ³)	2452.8(8)	5473.07(8)	1674.5(14)	6136(3)
<i>D</i> _{calcd} (g cm ⁻³)	1.236	1.174	1.118	1.173
<i>Z</i>	4	8	2	8
abs coeff, μ , mm ⁻¹	0.638	0.387	0.393	0.439
no. of data collected	12 066	25 063	7166	11 100
no. of data $F_o^2 > 3\sigma(F_o^2)$	4284	4794	4749	6168
no. of variables	235	289	325	608
<i>R</i> (%)	0.0375	0.0874	0.0412	0.0655
<i>R</i> _w (%)	0.0980	0.2115	0.1078	0.1515
goodness of fit	1.057	1.022	1.029	0.945

^a All data collected at 24 °C with Mo K α radiation ($\lambda = 0.71069$ Å), $R = \sum |F_o| - |F_c| / \sum |F_o|$, $R_w = [\sum [w(F_o^2 - F_c^2)^2] / \sum [wF_o^2]^2]^{0.5}$.

cyclopentadienyl substituents in **27** and **28** are oriented away from the phosphinimide ligand, presumably reflecting a preferred geometry in which steric conflicts are minimized.

The key metric parameters for these structures are presented in Table 3. In each case, the geometry about the N atom is approximately linear with the P–N–Ti angles ranging between 159.6(2)° and 176.6(4)°. The P–N and Ti–N distances are very similar in all these compounds, averaging 1.606(7) and 1.758(14) Å, respectively. Similarly, the Cl–Ti–Cl and N–Ti–Cl angles

vary only slightly, averaging 102.6(10)° and 102.4(8)°, respectively. The angles at Ti between the centroid of the η^5 -carbons of the Cp-type ligands and N appear to reflect the steric demands of both ligands. For compounds **11**–**13** the N–Ti–Cp angles range from 116.1° for the *i*-Pr₃PN derivative to 122.0° for the *t*-Bu₃PN species. For compounds **27** and **28** this angle is similar to that seen for **13**; however it increases to 125.3° for compound **22**, consistent with the steric influence of the substituted cyclopentadienyl ligand. Similarly, the N–Ti–Cp angle in **23** of 120.3° is significantly higher

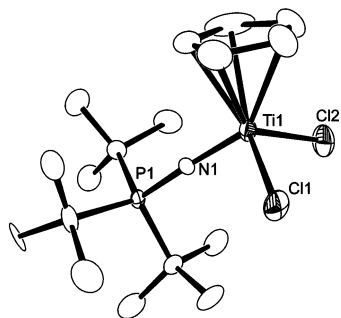


Figure 1. ORTEP drawing of **13**, 30% thermal ellipsoids, H atoms omitted for clarity.

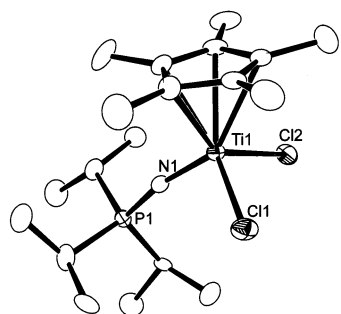


Figure 2. ORTEP drawing of **21**, 30% thermal ellipsoids, H atoms omitted for clarity.

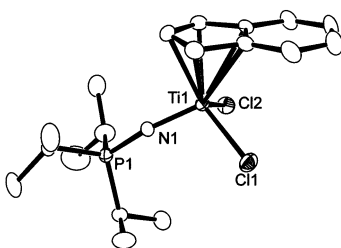


Figure 3. ORTEP drawing of **23**, 30% thermal ellipsoids, H atoms omitted for clarity.

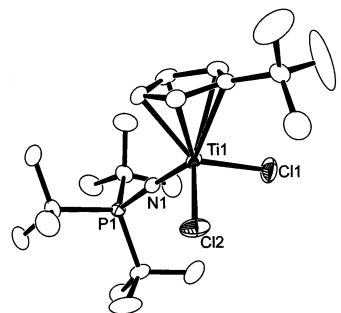


Figure 4. ORTEP drawing of **27**, 30% thermal ellipsoids, H atoms omitted for clarity.

than that found in **12** (116.1°), again reflecting what is predominantly a steric influence of indenyl versus cyclopentadienyl ligands.

The reactions of the above precursors with 2 equiv of MeLi proceed, in general, in high yields, providing a facile route to the series of compounds of the form $\text{CpTi}(\text{NPR}_3)_2\text{Me}_2$ and $\text{Cp}^*\text{Ti}(\text{NPR}_3)_2\text{Me}_2$ (Table 1). In a similar fashion, reactions with benzyl-Grignard reagents afford *bis*-benzyl derivatives, $\text{CpTi}(\text{NPR}_3)_2\text{Bn}_2$ ($\text{R} = \text{Cy}$ **46**, *i*-Pr **47**, *t*-Bu **48**, Ph **49**, *p*-MeC₆H₄ **50**, *p*-CF₃C₆H₄ **51**, *p*-FC₆H₄ **52**, *p*-MeOC₆H₄ **53**) in high yield. Arylation using PhLi or related substituted Grignard reagents also proceeds efficiently to give the compounds **54–60**

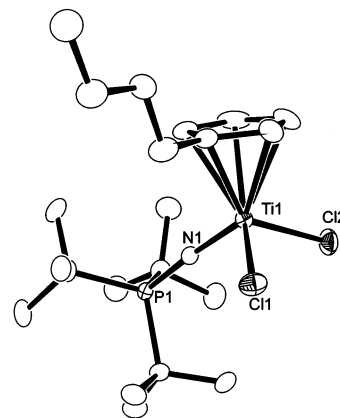


Figure 5. ORTEP drawing of **28**, 30% thermal ellipsoids, H atoms omitted for clarity.

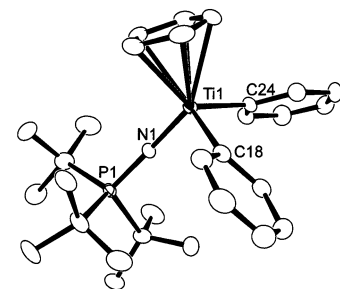


Figure 6. ORTEP drawing of **56**, 30% thermal ellipsoids, H atoms omitted for clarity. Ti(1)–N(1) 1.783(3) Å, Ti(1)–C(24) 2.128(5) Å, Ti(1)–C(18) 2.170(5) Å, N(1)–P(1) 1.602(4) Å; Ti(1)–N(1)–P(1) 169.4(3)°, N(1)–Ti(1)–C(24) 105.27(18)°, N(1)–Ti(1)–C(18) 99.87(18)°.

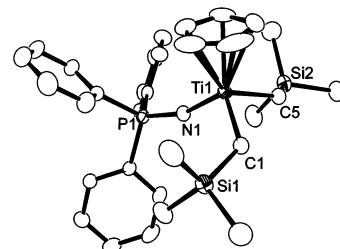


Figure 7. ORTEP drawing of **62**, 30% thermal ellipsoids, H atoms omitted for clarity. Ti(1)–N(1) 1.814(2) Å, Ti(1)–C(5) 2.128(3) Å, Ti(1)–C(1) 2.139(3) Å, P(1)–N(1) 1.581(2) Å, N(1)–Ti(1)–C(1) 104.05(11)°, C(5)–Ti(1)–C(1) 97.34(12)°, P(1)–N(1)–Ti(1) 160.44(15)°.

(Table 1, Scheme 1). As a final example, the species $\text{CpTi}(\text{NPR}_3)_2(\text{CH}_2\text{SiMe}_3)_2$ ($\text{R} = \textit{t}-Bu **61**, Ph **62**) was readily obtained in 83% yield via the reaction of **13** and **14** with the alkylating agent $(\text{CH}_3)_3\text{SiCH}_2\text{MgCl}$. For all of alkyl/aryl derivatives, full spectroscopic characterizations were consistent with the formulations.$

X-ray crystallographic data were also obtained for compounds **56** (Figure 6) and **61** (Figure 7). The structures of compounds **56** and **62** are as expected. The Ti–N distance in **56** of 1.783(3) Å is only slightly longer than that seen in **13**, whereas the corresponding distance in **62** is significantly longer (1.814(2) Å). This reflects the differing donor abilities of both the alkyl and aryl groups as well as that of the phosphinimide ligands. The P–N–Ti angle in **56**, $169.4(2)^\circ$, falls in the range observed for the complexes above. On the other hand, the smaller P–N–Ti angle ($160.44(15)^\circ$) and the shorter P–N distance (1.581(2) Å) in **62** reflect the poorer donor

Table 3. Metric Parameters^a for Compounds of the Form (Cp')Ti(NPR₃)Cl₂

cmpd	Ti–Cl	Ti–N	N–P	Cl–Ti–Cl	N–Ti–Cl _{av}	Ti–N–P	N–Ti–Cp ^b
11	2.3074(9)	1.755(2)	1.606(2)	102.12(4)	103.43(8)	172.02(15)	121.3
	2.3098(9)				102.55(8)		
12	2.2928(14)	1.750(3)	1.609(3)	102.07(6)	102.79(10)	169.84(19)	116.1
	2.3015(13)				102.67(10)		
	2.2945(13)	1.750(3)	1.616(3)	101.66(5)	103.39(10)	167.24(19)	
	2.3020(12)				103.73(10)		
13	2.309(3)	1.775(11)	1.593(10)	102.69(12)	102.6(2)	176.6(4)	122.0
	2.313(12)				102.7(2)		
21	2.299(3)	1.759(4)	1.608(4)	102.14(10)	102.8(2)	167.8(4)	122.6
	2.314(2)				101.86(17)		
22	2.3050(18)	1.794(3)	1.595(3)	100.70(7)	101.68(11)	165.5(2)	125.3
	2.3204(15)				102.56(10)		
23	2.2932(14)	1.741(4)	1.611(4)	102.96(6)	104.20(13)	159.6(2)	120.3
	2.3067(12)				101.61(11)		
	2.2968(13)	1.746(4)	1.600(4)	103.68(5)	103.73(12)	163.9(2)	
	2.3021(13)				101.31(11)		
27	2.3096(10)	1.761(2)	1.612(2)	103.42(5)	101.72(8)	176.28(15)	122.3
	2.3148(11)				101.84(8)		
28	2.3114(8)	1.7587(18)	1.6033(19)	102.13(3)	101.65(6)	175.91(12)	122.3
	2.3162(9)				102.55(7)		

^a Where two set of parameters are reported, the structural data reveal two molecules in the asymmetric unit; errors in parentheses are the standard deviations computed on the basis of the five bond lengths. ^b N–Ti–Cp angles refer to the angle at Ti between N and the centroid of the five η^5 -carbons.

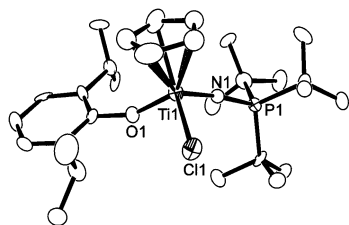


Figure 8. ORTEP drawing **63** (one of the two molecules in the asymmetric unit), 30% thermal ellipsoids, H atoms omitted for clarity. Ti(1)–N(1) 1.775(9) Å, Ti(1)–O(1) 1.846(8) Å, Ti(1)–Cl(1) 2.339(4) Å, P(1)–N(1) 1.588(10) Å, N(1)–Ti(1)–O(1) 104.1(4)°, N(1)–Ti(1)–Cl(1) 101.5(3)°, O(1)–Ti(1)–Cl(1) 101.9(3)°, P(1)–N(1)–Ti(1) 170.9(7)°, C(6)–O(1)–Ti(1) 153.3(8)°.

ability of the Ph₃PN ligand. The C(18)–Ti–C(24) angle of 101.48(19)° in **56** and the C(5)–Ti–C(1) angle of 97.34(12)° in **61** are smaller than the Cl–Ti–Cl angles described above. The Ti–C bond lengths (2.128(5), 2.170(5) Å) in **56** are significantly shorter than those seen in Cp₂TiPh₂ (2.272(14) Å)⁵⁴ but similar to those seen in **61** (2.128(3), 2.139(3) Å). This presumably reflects the electron-deficient nature of the Ti center in these compounds relative to that in the corresponding titanocene.

Substitution of one of the chloride ligands of **13** was also achieved by direct reaction with the bulky aryloxide salt Na[O-2,6-(*i*-Pr)₂C₆H₃]. In this manner, the species CpTi(NP(*t*-Bu)₃)Cl(O-2,6-*i*-Pr₂C₆H₃), **63**, was obtained in 96% yield. The spectroscopic data confirmed the formulation as well as the diastereotopic nature of the isopropyl methyl groups. A crystallographic study of **63** (Figure 8) revealed Ti–N and Ti–O distances of 1.775(9) and 1.846(8) Å, respectively, with P–N–Ti and C–O–Ti angles of 170.9(7)° and 153.3(8)°, suggesting that phosphinimide is a stronger π -donor than the aryloxide.

Ethylene Polymerization. The synthetic chemistry above provides facile access to a large series of related Ti complexes. This offers an opportunity to probe

structure–activity correlations in olefin polymerization. Polymerization of ethylene was examined initially in small-scale Schlenk line catalyst screening experiments.

Compounds **11–31** were employed as catalyst precursors using 500 equiv of methylalumoxane (MAO) as the activator (Table 4). In general, these catalysts exhibit single site activity, as evidenced by the relatively narrow polydispersities of the resulting polyethylene (PE). However, the PE derived from compounds **11**, **12**, **25**, and **26** show bimodal distributions of molecular weights, suggesting the presence of more than one active site. It is noteworthy that in these cases although these catalysts have reduced activity, M_w 's of PE as high as 9×10^5 g/mol were observed.

The catalysts derived from compounds **14–18** permit examination of electronic factors, as these species are essentially isosteric. The observed differences in activity are relatively small, but the trend suggests that electron-donating substituents favor somewhat higher activities. On the other hand, the catalysts derived from **10–13** are electronically similar, although the steric demands of the ancillary phosphinimide ligand vary significantly. The observed activities in these cases infer marked dependence on steric factors, as all of the tri-*tert*-butylphosphinimide complexes **13**, **20**, **27**, **44**, and **62** showed activities that are comparable to those observed for Cp₂ZrCl₂ and the constrained geometry catalyst [(C₅-Me₄SiMe₂N-*t*-Bu)TiCl₂] (CGC). Also, they are significantly higher than those observed for Cp₂TiCl₂ or CpTiCl₃ using the same apparatus and conditions. In contrast the catalysts derived from the smaller phosphinimide ligands exhibit markedly reduced activity. GPC data for the PE derived for the active systems reveal average M_w from 55 000 to 203 500 with polydispersities of 1.6–2.4.

Initial small-scale Schlenk line screenings were performed employing dimethyl complexes **30–32** and **42–44** as catalyst precursors and using [Ph₃C][B(C₆F₅)₄] as the activator. These phosphinimide-based catalysts rapidly generate high molecular weight, highly linear (by NMR) polyethylene. The polymer generated from complexes **30–32** range in M_w from 135 000 to 165 000

(54) Kocman, V.; Rucklidge, J. C. *Chem. Commun.* **1971**, 1340.

Table 4. Ethylene Polymerization Screening Data

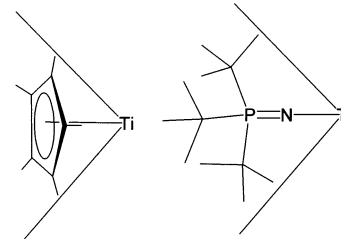
pre-cat.	co-cat. ^a	activity ^a	M_w^b	PDI ^e	pre-cat.	co-cat. ^a	activity ^a	M_w^b	PDI ^e
10	MAO/a	13			23	MAO/a	28		
11	MAO/a	42	3590	1.8	24	MAO/a	425		
			336 000	2.2					
12	MAO/a	49	18 700	2.8	25	MAO/a	46	7410	2.1
			578 500	2.4				893 500	3.4
13	MAO/a	652	89 900	1.6	26	MAO/a	16	7580	1.9
								910 200	2.5
14	MAO/a	34	109 200	2.6	27	MAO/a	881	65 400	2.4
15	MAO/a	35			28	MAO/a	2000		
16	MAO/a	31			44	MAO/a	853	55 600	2.3
17	MAO/a	34			61	MAO/b	300	81 400	3.6
18	MAO/a	47			62	MAO/a	765	203 500	1.9
19	MAO/a	16			Cp ₂ ZrCl ₂	MAO/a	895	116 353	2.8
20	MAO/a	494	135 800	1.7	CGC ^d	MAO/a	630		
21	MAO/a	30			Cp ₂ TiCl ₂	MAO/a	415		
22	MAO/a	1400			CpTiCl ₃	MAO/a	<10		
30	TB/a	231	134 600	2.8	Cp ₂ ZrCl ₂	MAO/c	670	340 800	2.1
31	TB/a	225	163 800	3.9	42	TB/a	1807	310 200	7.5 ^c
32	TB/a	401	165 800	3.4	43	TB/a	1193	259 200	9.9 ^c
32	MAO/c	830	812 000	1.7	44	TB/a	1296	321 300	12.3 ^c
32	TMA/c	<1			13	MAO/c	1485		

^a MAO, methylalumoxane (500 equiv); TB, trityl tetrakis(pentafluorophenyl)borate (2 equiv); TMA, trimethylaluminum. Activity reported in g/mmol/h/atm. Conditions: (a) Schlenk line, 1 atm pressure of ethylene and 25 °C, 5 min. (b) Schlenk line, 1 atm pressure of ethylene and 25 °C, 30 min. (c) Büchi reactor, 1.8 atm pressure of ethylene, 30 °C, 30 min. ^b Molecular weight data were recorded against polyethylene standards. ^c The high activity of these systems together with the observation of polydispersities in the range 7–12 suggest that these polymerizations rapidly become diffusion-controlled reactions. ^d CGC = [(C₅Me₄SiMe₂N-*t*-Bu)TiCl₂]. ^e Where two MWs are reported, GPC curves were clearly bimodal and the quoted polydispersities were derived from a computational fit.

g/mol with polydispersities in the range of 2.4–3.8. The catalysts derived from analogous *tert*-butylcyclopentadienyl complexes **42–44** and trityl-borate activation gave even higher molecular weight polyethylene (M_w : 260–320 000). Moreover it was very encouraging to note that the activities of the latter systems were as much as twice that derived from Cp₂ZrCl₂ and three times that derived from the CGC, under similar conditions.

Selected cases were scaled up for testing on a Büchi reactor. In this system, typically 600–700 mL of solvent was employed with catalyst concentrations of approximately 50 μmol/L while the ethylene pressure was around 1.8 atm. The trials reported here are 30 min, and the active catalysts produce 10–20 g of PE. In this manner, catalysts derived from compounds **13** and **32** with MAO activation showed activity of 1485 and 830 g PE/mmol/h/atm, respectively. Interestingly, changes to the Al activator had dramatic effects. Replacing MAO with AlMe₃ results in a dramatic plummet in activity. We have recently described reactions of CpTi(NPR₃)Me₂ with AlMe₃ which proceed through a series of C–H activation reactions, ultimately affording Ti–Al–carbide aggregates.^{49,55–58} This chemistry may account for the dramatic reduction in activity of these catalysts in the presence of AlMe₃.

Catalyst Design Considerations. The results above demonstrate that the family of compounds of the form (Cp')TiX₂(NPR₃) are effective catalyst precursors for olefin polymerization. The original concept on which these developments were based was the notion of a steric analogy between cyclopentadienyl and phosphin-

Scheme 2

imide ligands, though clearly this notion is fraught with limitations. However, from the above structural data, the maximum angle subtended at Ti or the “cone angle”^{59,60} for the phosphinimide ligand, *t*-Bu₃PN, was determined to be approximately 87°, similar to that observed for a metal-bound cyclopentadienyl ligand (83°) (Scheme 2). This suggests that these ligands occupy approximately similar volumes about the Ti center. On the other hand, it is clear that the steric bulk of a phosphinimide ligand is considerably removed from the metal as the Ti–P distance is over 3 Å, whereas the Ti–Cp-centroid distance is about 2.2 Å. The polymerization data also suggest that steric factors play a significant role in determining the effectiveness of a catalyst. For example, those catalysts incorporating *tert*-butylphosphinimide ligands as in **13**, **20**, **22**, **24**, **27**, and **28** are in general quite active. On the other hand, for the systems where additional substitution on the cyclopentadienyl ligand contributes to the definition of the active site, sterically less demanding phosphinimide ligands still provide for high activity. Examples of this latter situation are the catalysts derived from compounds **42** and **43**. These polymerization data suggest that the general strategy of employing ancillary ligands with similar steric bulk to cyclopentadienyl ligands has some viability. On the other hand, it also reveals

(55) Guerin, F.; Stephan, D. W. *Angew. Chem., Int. Ed.* **1999**, *38*, 3698–3701.

(56) Kickham, J. E.; Guerin, F.; Stewart, J. C.; Stephan, D. W. *Angew. Chem., Int. Ed.* **2000**, *39*, 3263–3266.

(57) Kickham, J. E.; Guerin, F.; Stewart, J. C.; Urbanska, E.; Ong, C. M.; Stephan, D. W. *Organometallics* **2001**, *20*, 1175–1182.

(58) Yue, N.; Hollink, E.; Guérin, F.; Stephan, D. W. *Organometallics* **2001**, *20*, 4424–4433.

(59) Tolman, C. A. *J. Am. Chem. Soc.* **1970**, *92*, 2956–2965.

(60) Tolman, C. A. *Chem. Rev.* **1977**, *77*, 313–348.

limitations of this approach, in that the very subtle changes to the steric demands result in major changes in activity. Although these subtleties are not well understood, it is thought that the role of steric congestion is to preclude deactivation pathways, including cation dimerization and interaction with Lewis acids leading to C–H activation. We have identified these pathways in related phosphinimide complex systems.^{56,58,61,62}

It is perhaps surprising that the complexes described herein are highly effective catalysts, given the similar success associated with the CGC. While both systems provide a cyclopentadienyl- and N-based ligand to the Ti center, the Cp-centroid–Ti–N angles (Table 3) in the present phosphinimide complexes are significantly greater than that found in the CGC (107.6°).⁴³ This seems to counter the notion that increased exposure of the Ti center is required for heightened reactivity.

The electronic character of phosphinimide ligands has been previously probed by Dehnicke and co-workers.^{45–48} The σ – π^2 nature of the interaction with a metal center suggests an electronic analogy to a cyclopentadienyl ligand as well. Nonetheless the present polymerization data demonstrate that minor perturbations to the donor ability of the phosphinimide alter the activity of the resulting catalysts to a small extent. However, it is noteworthy that this comparison is made among cata-

lysts that operate in a low-activity regime. It may be that electronic effects would be more dramatic for higher activity systems. This aspect is the subject of ongoing synthetic efforts.

In summary, the feasibility of an approach to catalyst design based on the steric analogy between phosphinimide and cyclopentadienyl ligands is supported by the family of titanium phosphinimide complexes (Cp[†])TiX₂(NPR₃). Both the demonstrated activity of these species in olefin polymerization and the metric parameters of the titanium-phosphinimide complexes support the view that such ligands provide a metal environment that mimics metallocenes to some extent. Among the present systems, it appears that steric rather than electronic factors are key to the generation of highly active systems. The optimization of the catalyst structure for activity continues to be one focus of our efforts. Efforts to apply these systems to a variety of other processes are also the subjects of ongoing studies.

Acknowledgment. Financial support from the NSERC of Canada and NOVA Chemicals Corporation is gratefully acknowledged. Thanks to Keith Christall for the synthesis of **28**. D.W.S. is grateful to the Alexander von Humboldt Stiftung for the award of a Forschungpreis.

Supporting Information Available: Crystallographic information tables as well as ORTEP drawings of all structures reported herein. This material is available free of charge via the Internet at <http://pubs.acs.org>.

OM020954T

(61) Yue, N. L. S.; Stephan, D. W. *Organometallics* **2001**, *20*, 2303–2308.

(62) Kickham, J. E.; Guerin, F.; Stewart, J. C.; Urbanska, E.; Ong, C. M.; Stephan, D. W. *Organometallics* **2001**, *20*, 3209.